CrystEngComm

Accepted Manuscript

ROYAL SOCIETY OF CHEMISTRY

www.rsc.org/crystengcomm

Journal Name

ARTICLE

Enhanced Catalytic Activity of a Hierarchical Porous Metal-Organic Framework CuBTC

Received 00th January 20xx,
Accepted 00th January 20xx

DOI: 10.1039/x0xx00000x

www.rsc.org/

Zhigang Hu, Yongwu Peng, Kai Min Tan, and Dan Zhao*

A previously reported mixed ligand strategy was used to synthesize a classic metal-organic framework CuBTC, which exhibited a hierarchical porous structure including micropores and mesopores of around 3.9 nm. Thanks to facile mass transfer and denser open metal sites induced by mixed ligand strategy, the hierarchical porous CuBTC demonstrates enhanced catalytic activity towards both ring-opening reaction of styrene oxide to 2-methoxy-2-phenylethanol and cyanosilylation reaction of benzaldehyde to cyanohydrins.

Introduction

Metal-organic frameworks (MOFs), also known as porous coordination polymers (PCPs), have become one of the most exciting porous crystalline materials nowadays.[1-3] Possessing tunable porosity and rich chemical functionalities, MOFs have been widely explored in applications such as storage,[4, 5] separation,[6, 7] sensing,[8-10] catalysis,[11, 12] etc. To date, most of the reported MOFs are microporous, with pore sizes less than 2 nm.[13] The relatively small pore size of MOFs has limited their applications in heterogeneous catalysis, where mesopores (pore size between 2 and 50 nm) are normally preferred for increased mass transfer.[14] For example, CuBTC (aka HKUST-1) is a classic MOF composed of benzenetricarboxylate (BTC) ligand with dicopper paddlewheel secondary building units (SBUs) that has been extensively studied due to its facile synthesis and potential commercialization.[15-17] The solvent molecules binding to the SBUs of CuBTC can be removed affording open metal sites that can serve as hard Lewis acid for heterogeneous catalysis.[18-23] However, its catalytic ability toward large substrates is greatly limited by its microporous structure with window openings of only *ca.* 6 Å in diameter that prevent the diffusion of large substrates. Several approaches have been reported to introduce mesoporosity into MOFs,[24-26] such as crystal engineering,[27-30] ligand extension,[31-33] template-assisted synthesis,[34-38] post-synthetic modification,[39, 40] mechanochemical synthesis,[41] etc. In principle, the relatively week coordination bonds in MOFs can be twisted, broken, and reconstructed leading to MOFs of interesting and useful properties.[42] Recently, Zhou *et al.* reported a truncated ligand strategy by mixing symmetric ligands with reduced symmetric ligands to synthesize isostructural MOFs with enlarged pore size.[43, 44] A similar strategy was used by Barin *et al.* in creating defects in CuBTC.[45] In their study, increased pore volume and surface area were observed in CuBTC upon fragment ligand incorporation, but the pore size remained more or less unchanged. Marx *et al.* used the mixed ligand strategy to introduce catalytically active functional groups into CuBTC.[46] In another study done by Fang *et al.*, extra open Cu sites as well as hierarchical porosity including micropores and mesopores were introduced into CuBTC frameworks by mixing BTC ligand with defective linkers.[47]

In view of the above results, we herein report a facile synthesis of hierarchical porous CuBTC (Scheme 1), which was achieved similarly by introducing an asymmetric ligand (isophthalic acid, IPA) but with a different synthetic condition compared to the work of Barin *et al.*[45] The resultant hierarchical porous CuBTC exhibited microporous structure as well as mesoporous texture with pore sizes as large as 3.9 nm. In addition, the effect of hierarchical porosity on catalytic performance was studied. Compared to pristine CuBTC, the hierarchical porous one demonstrates a much higher catalytic activity towards both ring opening reaction of styrene oxide to 2-methoxy-2-phenylethanol and cyanosilylation reaction of benzaldehyde to cyanohydrins, which can be attributed to facilitated mass transfer in mesopores and denser Lewis acid sites.

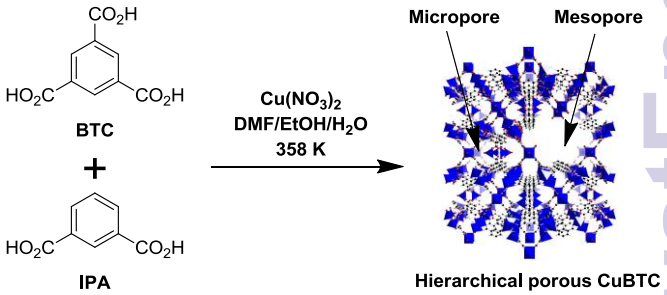

Scheme 1. Synthetic scheme of hierarchical porous CuBTC using truncated mixed ligand strategy.

Department of Chemical and Biomolecular Engineering, National University of Singapore, Singapore 117585
E-mail: chezhao@nus.edu.sg

Experimental Section

Materials and methods

All of the reagents used were obtained from commercial suppliers and used without further purification. Powder X-ray diffraction (PXRD) patterns were obtained on a Bruker D8 Advance X-ray powder diffractometer equipped with a Cu sealed tube (λ = 1.54178 Å) at a scan rate of 0.02 deg s^{-1}. NMR data were collected on a Bruker Avance 500 MHz NMR spectrometer (DRX500). Field-emission scanning electron microscope (FE-SEM) analyses were conducted on an FEI Quanta 600 SEM (20 kV) equipped with an energy dispersive spectrometer (EDS, Oxford Instruments, 80 mm2 detector). Samples were treated via Pt sputtering before observation.

Synthetic procedures

The hierarchical porous CuBTC (referred to as HP-CuBTC) samples were synthesized by revising a reported method.[45] Briefly, mixtures of benzene-tricarboxylic acid (BTC, 100 mg, 0.51 mmol) and copper nitrate trihydrate [$Cu(NO_3)_2{\cdot}3H_2O$, 200 mg, 0.82 mmol] together with different ratios of isophthalic acid (IPA, 0.5, 1, 2, and 4 equivalent mole of BTC, namely 40, 80, 160, and 320 mg) were dissolved in 20 ml of mixed solvents containing dimethylformamide (DMF)/ethanol/water (1:1:1 v/v/v). The solutions were sonicated for 30 min and then heated at 85 °C for 20 h. The solid products were recovered by centrifuge, washed with DMF for three times, and then soaked in DMF at 80 °C for 24 h to completely remove any un-reacted ligands trapped inside the frameworks. The samples then underwent solvent exchange with methanol for three days, and were fully activated at 120 °C under vacuum for 24 h.

Gas sorption measurements

Gas sorption isotherms were measured up to 1 bar using a Micromeritics ASAP 2020 surface area and pore size analyzer. Before the measurements, samples (*ca.* 100 mg) were degassed under reduced pressure (< 10^{-2} Pa) at 150 °C for 12 h. UHP grade He and N_2 were used for all the measurements. Oil-free vacuum pumps and oil-free pressure regulators were used to prevent contamination of the samples during degassing process and isotherm measurements. The temperature of 77 K was maintained with a liquid nitrogen bath. Pore size distribution data were calculated from the N_2 sorption isotherms at 77 K based on non-local density functional theory (NLDFT) model (assuming slit pore geometry) and Barrett-Joyner-Halenda (BJH) desorption model in the Micromeritics ASAP 2020 software package.

Catalytic reactions

Ring-opening reactions of styrene oxide with methanol catalyzed by either pristine CuBTC or HP-CuBTC were performed in closed vials heated at 40 °C under stirring. In specific, styrene oxide (150 mg, 1.25 mmol) was dissolved in methanol (5 ml), toward which 50 mg of activated MOFs (either pristine CuBTC or HP-CuBTC) was added. A certain amount of the reaction media (0.5 mL) was taken after 1, 2, and 3 h of reaction time and filtered, respectively. The filtrates were left dry and analyzed by NMR. Cyanosilylation reactions of benzaldehyde catalyzed with either pristine CuBTC or HP-CuBTC (15 mg) were carried out at a 1:2 molar ratio of benzaldehyde (0.3 mmol, 30 µl) and trimethylsilyl cyanide (TMSCN, 0.6 mmol, 80 µl) in dichloromethane (3 mL) at room temperature and 40 °C, respectively. A certain amount of the reaction media (0.5 mL) was taken after 12, 24, 36, and 48 h of reaction time and filtered, respectively. The filtrates were left dry and analyzed by NMR.

Results and Discussion

Structural characterization

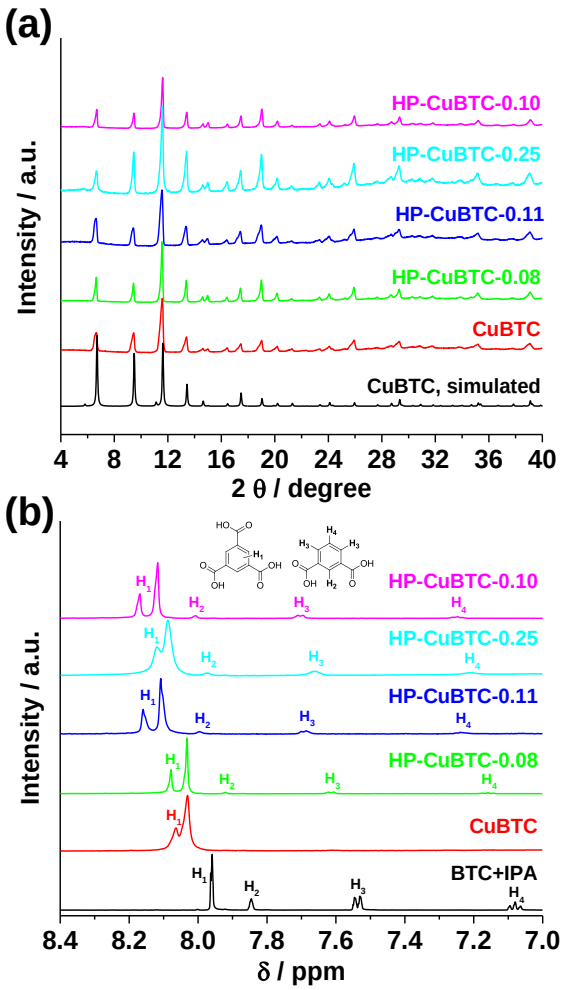

Figure 1. (a) PXRD patterns of simulated CuBTC, as-synthesized CuBTC, and HP-CuBTC samples obtained through mixed ligand strategy; (b) ^{1}H-NMR spectra of mixed ligands, CuBTC, and HP-CuBTC samples digested in D_2O/NaOH.

It is possible that the solvothermal reaction between copper nitrate and a mixed ligand of BTC and IPA can lead to phase impurities in resultant CuBTC because IPA alone can react with copper salt to give MOF products.[48] This possibility was ruled out in this study by checking the PXRD patterns of obtained HP-CuBTC samples. As can be seen from Figure 1a, all the HP-CuBTC samples exhibit similar PXRD patterns identical to that of pristine CuBTC and the one simulated from single crystal model of CuBTC, indicating that the resultant HP-CuBTC

samples have a framework connection identical to that of pristine CuBTC. This is probably because of the geometry similarity between IPA and BTC so that the overall CuBTC framework topology can still be maintained even after incorporation of IPA moieties.[43] FE-SEM images also revealed that HP-CuBTC crystals have a similar octahedral shape to that of pristine CuBTC (Figure 2).

The successful incorporation of IPA into HP-CuBTC was further confirmed by NMR spectra of digested MOFs (Figure 1b). The incorporated amount of IPA can be adjusted by applying different feed molar ratios of IPA to BTC. According to the integration of assigned peaks, the incorporated ratios are 0.08, 0.11, 0.25, and 0.10, for feed ratios of 0.5, 1, 2, and 4, respectively. Therefore, the resultant MOFs were named as HP-CuBTC_0.08, HP-CuBTC_0.11, HP-CuBTC_0.25, and HP-CuBTC_0.10, respectively. Surprisingly, the incorporated molar ratio of IPA didn't increase linearly with the increase of feed molar ratio, and there is a maximal incorporated ratio of 0.25 at a feed molar ratio of 2. A reduced incorporated ratio at higher feed ratio may be attributed to the role of crystal growth inhibitor played by IPA at high concentrations.[49, 50] It is worth noting that the NMR signal peaks from BTC in the digested MOF samples are split, possibly due to the different chemical environment of neutralized carboxylate moieties.

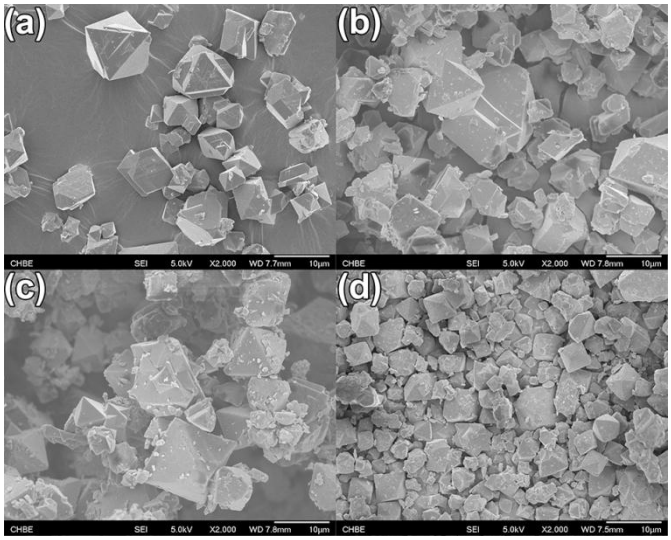

Figure 2. FE-SEM images of (a) CuBTC, (b) HP-CuBTC-0.08, (c) HP-CuBTC-0.11, and (d) HP-CuBTC-0.25. Scale bars represent 10 µm.

Surface area and pore size distribution

N_2 sorption data collected at 77 K and a pressure up to 1 bar were adopted to evaluate the surface areas of these samples using Brunauer–Emmett–Teller (BET) model (Figure 3a, Table 1). The pristine CuBTC synthesized in this study has a Type I isotherm indicating its microporous structure, with a BET specific surface area of 1690 $m^2 g^{-1}$ which is comparable to the reported values.[51, 52] With the increase of IPA incorporated into the frameworks, the isotherm of the products exhibited an increasingly distinct hybrid Type I/IV behavior featured by sharp increase of gas uptake at low pressures (Type I) and a H2-type hysteresis between adsorption and desorption branches at P/P_0 > 0.45 (Type IV).[13] Type IV isotherms are normally associated with mesoporosity confirming the increased pore size caused by IPA incorporation, and H2-type hysteresis indicates a presence of "bottleneck" pores with large cages accessible via small openings.[13] Indeed, theoretical study has predicted similar isotherms for hierarchical porous CuBTC.[53]

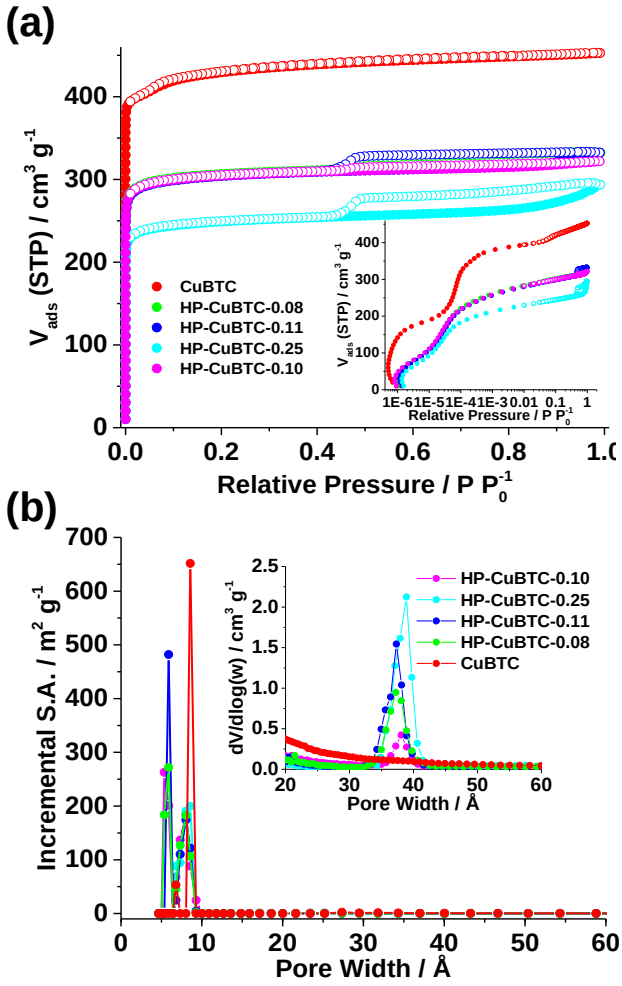

Figure 3. (a) N_2 sorption isotherms of CuBTC and HP-CuBTC. Closed and open symbols represent adsorption and desorption, respectively. The BET surface areas are also provided; (b) Pore size distribution data of CuBTC and HP-CuBTC calculated using NLDFT method (imbedded: pore size distribution data calculated using BJH desorption model).

In order to further confirm the hierarchical porosity, both NLDFT and BJH desorption models were applied to calculate the pore size distribution. As can be seen from the result of NLDFT calculation (Figure 3b), the pore size distribution of CuBTC is featured by two sizes of 8.6 Å (major) and 6.8 Å (minor), which matches quite well with the crystal structure. It is interesting to note that HP-CuBTC samples exhibit smaller pore sizes of *ca.* 5.7 Å (major) and *ca.* 8.0 Å (minor), possibly because of the introduction of truncated IPA moieties into the frameworks that make some of the pocket (e.g. the close

tetrahedron defined by four BTC moieties in CuBTC framework) accessible to probe gas molecules. BJH desorption models reveal that mesopores with pore size of *ca.* 3.9 nm were readily developed in HP-CuBTC samples, confirming their hierarchical porous structure containing both micropores and mesopores. Micropores are intrinsic for CuBTC-like crystal structure, while mesopores may come from ligand truncation[43, 44] and/or missing linker defects.[47] Considering the identical PXRD patterns of HP-CuBTC to pristine CuBTC, the mesopores in HP-CuBTC should be randomly distributed within the frameworks instead of being oriented in an ordered way.[36, 54]

Table 1. Summary of BET surface area (BET S.A.), micropore volume (micro. vol.) and mesopore volume (meso. vol.) of CuBTC and HP-CuBTC MOFs

MOFs	BET S.A.[a)]	Micro. Vol.[b)]	Meso. Vol.[c)]
CuBTC	1690	0.55	0.01
HP-CuBTC-0.08	970	0.39	0.03
HP-CuBTC-0.11	990	0.39	0.04
HP-CuBTC-0.25	930	0.30	0.07
HP-CuBTC-0.10	1000	0.39	0.02

[a)] $m^2\ g^{-1}$; [b)] $d_{pore} < 20$ Å, $cm^3\ g^{-1}$, NLDFT; [c)] 20 Å < d_{pore} < 1000 Å, $cm^3\ g^{-1}$, NLDFT.

Catalytic performance study

Larger pore sizes are supposed to facilitate the mass transfer of substrates within porous structures which is highly beneficial for heterogeneous catalysis.[14, 55] Theoretical calculation also reveals that molecular diffusion in mesopores is faster than in micropores of MOFs.[53] Considering that HP-CuBTC_0.25 has open copper sites as Lewis acid with mesopores of about 3.9 nm, we chose two model reactions that can be catalyzed by Lewis acid to study the impact of hierarchical porosity on the catalytic performance of MOFs. The first model reaction is ring-opening reaction of styrene oxide with methanol to 2-methoxy-2-phenylethanol, with the product being a very important organic solvent and reaction intermediate in pharmaceutical industry.[56] Reactions were carried out at 40 °C according to the literature with either HP-CuBTC-0.25 or pristine CuBTC as the catalyst.[36] After 4 h of reaction, HP-CuBTC-0.25 showed a much higher conversion (35.6 %) than that of pristine CuBTC (1.97 %) (Figure 4a). This result strongly demonstrates the benefits brought by hierarchical porosity in heterogeneous catalysis. However, we noticed that the crystallinity of HP-CuBTC-0.25 was retained after first catalysis reaction but was lost during second catalytic cycle. The reason is that CuBTC is an intrinsically unstable MOF composed of Cu-O bonds that are susceptible to the attack of guest molecules, which has been demonstrated previously.[18] The second model reaction we have attempted is cyanosilylation of benzaldehyde into cyanohydrins. Reactions were carried out at a 1:2 molar ratio of benzaldehyde to trimethylsilyl cyanide (TMSCN) in dichloromethane (DCM, 3 mL) at either 298 K or 313 K according to the literature.[57] A loading of 5 mol% MOF catalyst and reaction time of 48 h was adopted herein for convenient compare with the literature value.[18, 58] Incubation of benzaldehyde and TMSCN with pristine CuBTC as the catalyst at 313 K for 48 h led to a conversion of 56.4% (Figure 4b), which is similar to the reported value of *ca.* 50%.[18, 58] However, this reaction is relatively sluggish, with a conversion of only 8.4% within the first 12 h of reaction time. When HP-CuBTC-0.25 was used as the catalyst, a substantially increased conversion of 45.6% was observed under the same reaction time, indicating much faster reaction kinetics. After 48 h, 64.2 % of benzaldehyde was converted to cyanohydrins catalyzed by HP-CuBTC-0.25, which is also higher than the reaction catalyzed by pristine CuBTC (56.4 %). However, we have to point out that the MOF catalysts in this study survived after 36 h of reaction time, but completely dissolved after 48 h indicating their instability under this reaction condition.[18] Similar finding was reported by Opanasenko *et al*.[21, 22] In order to evaluate MOFs' catalytic performance under a milder condition, similar catalytic reactions were carried out at a lower temperature of 298 K. Once again, HP-CuBTC-0.25 exhibited a much higher conversion (34.5%) than that of pristine CuBTC (10.8%) after 20 h of reaction time.

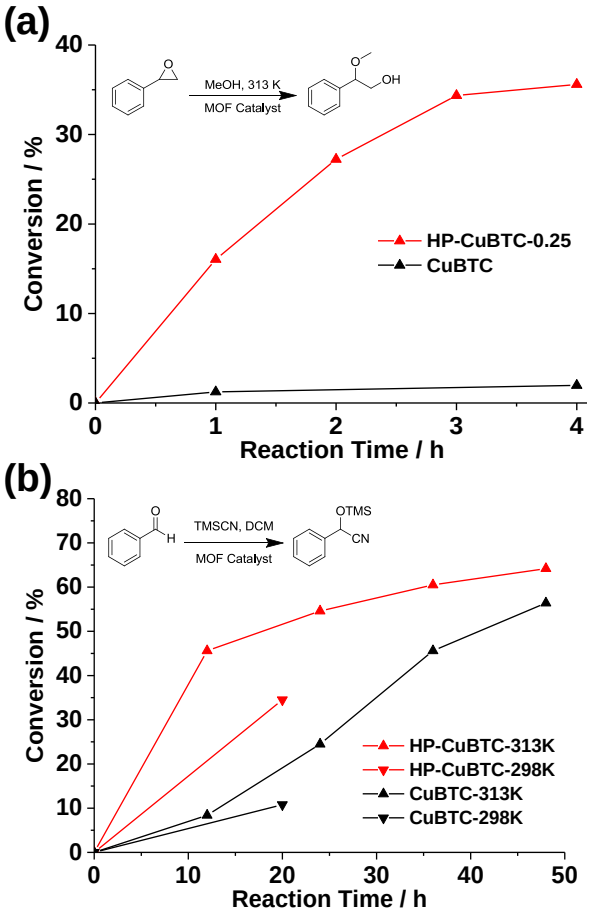

Figure 4. (a) Ring-opening reaction of styrene oxide with methanol to 2-methoxy-2-phenylethanol catalyzed by CuBTC or HP-CuBTC-0.25 at 313 K; (b) cyanosilylation of benzaldehyde into cyanohydrins catalyzed by CuBTC or HP-CuBTC-0.25 at 298 and 313 K, respectively.

The above two model reactions have clearly indicated enhanced catalytic activities of HP-CuBTC compared to pristine CuBTC. One reason could be the mesopores introduced within HP-CuBTC that facilitate the substrate transport and make it easier to get access to catalytically active open Cu sites. In addition, several studies have confirmed that extra open metal sites can be generated through missing linker defects.[47, 59, 60] It is possible that the truncated ligand strategy used in this study may generate extra open Cu sites which also help the catalysis. Eventually, it might be a synergetic effect involving hierarchical porosity and denser open metal sites that contributes to the enhanced catalytic activities. Nevertheless, we have to point out that due to a lack of quantitative measurement of decomposition of Cu-MOFs and solid evidence to prove the reaction is completely heterogeneous, a homogeneous mechanism involving leached copper ions could also be possible for the enhanced catalytic performance.

Conclusions

In summary, we have applied truncated mixed ligand strategy to synthesize hierarchical porous CuBTC exhibiting both micropores and mesopores up to 3.9 nm. Compared to pristine CuBTC, HP-CuBTC-0.25 demonstrates a much better catalytic performance towards both ring-opening reaction of styrene oxide to 2-methoxy-2-phenylethanol and cyanosilylation reaction of benzaldehyde to cyanohydrins. The strategy demonstrated in this study may be applied to other MOFs towards mesoporous MOFs for heterogeneous catalysis applications.

Acknowledgements

This work is supported by National University of Singapore (NUS Start-up Funding R-279-000-369-133, CENGas R-261-508-001-646) and Singapore Ministry of Education (MOE AcRF Tier 1 R-279-000-410-112, AcRF Tier 2 R-279-000-429-112).

Notes and references

1. J. R. Long and O. M. Yaghi, *Chem. Soc. Rev.*, 2009, **38**, 1213-1214.
2. H. C. Zhou, J. R. Long and O. M. Yaghi, *Chem. Rev.*, 2012, **112**, 673-674.
3. H. C. Zhou and S. Kitagawa, *Chem. Soc. Rev.*, 2014, **43**, 5415-5418.
4. D. Zhao, D. Q. Yuan and H. C. Zhou, *Energy Environ. Sci.*, 2008, **1**, 222-235.
5. M. P. Suh, H. J. Park, T. K. Prasad and D. W. Lim, *Chem. Rev.*, 2012, **112**, 782-835.
6. J. R. Li, J. Sculley and H. C. Zhou, *Chem. Rev.*, 2012, **112**, 869-932.
7. K. Sumida, D. L. Rogow, J. A. Mason, T. M. McDonald, E. D. Bloch, Z. R. Herm, T. H. Bae and J. R. Long, *Chem. Rev.*, 2012, **112**, 724-781.
8. M. D. Allendorf, C. A. Bauer, R. K. Bhakta and R. J. T. Houk, *Chem. Soc. Rev.*, 2009, **38**, 1330-1352.
9. Y. J. Cui, Y. F. Yue, G. D. Qian and B. L. Chen, *Chem. Rev.*, 2012, **112**, 1126-1162.
10. M. Zhang, G. X. Feng, Z. G. Song, Y. P. Zhou, H. Y. Chao, D. Q. Yuan, T. T. Y. Tan, Z. G. Guo, Z. G. Hu, B. Z. Tang, B. Liu and D. Zhao, *J. Am. Chem. Soc.*, 2014, **136**, 7241-7244.
11. J. Lee, O. K. Farha, J. Roberts, K. A. Scheidt, S. T. Nguyen and J. T. Hupp, *Chem. Soc. Rev.*, 2009, **38**, 1450-1459.
12. A. Corma, H. Garcia and F. X. L. Xamena, *Chem. Rev.*, 2010, **110**, 4606-4655.
13. K. S. W. Sing, D. H. Everett, R. A. W. Haul, L. Moscou, R. A. Pierotti, J. Rouquérol and T. Siemieniewska, *Pure Appl. Chem.*, 1985, **57**, 603-619.
14. A. Taguchi and F. Schüth, *Microporous Mesoporous Mat.*, 2005, **77**, 1-45.
15. S. S. Y. Chui, S. M. F. Lo, J. P. H. Charmant, A. G. Orpen and I. D. Williams, *Science*, 1999, **283**, 1148-1150.
16. U. Mueller, M. Schubert, F. Teich, H. Puetter, K. Schierle-Arndt and J. Pastré, *J. Mater. Chem.*, 2006, **16**, 626-636.
17. A. U. Czaja, N. Trukhan and U. Müller, *Chem. Soc. Re* 2009, **38**, 1284-1293.
18. K. Schlichte, T. Kratzke and S. Kaskel, *Microporou Mesoporous Mat.*, 2004, **73**, 81-88.
19. L. Alaerts, E. Séguin, H. Poelman, F. Thibault-Starzyk, P. A. Jacobs and D. E. De Vos, *Chem.-Eur. J.*, 2006, **12**, 7353-7363.
20. A. Dhakshinamoorthy, M. Alvaro and H. Garcia, *Chem. Commun.*, 2012, **48**, 11275-11288.
21. M. Opanasenko, M. Shamzhy and J. Čejka, *ChemCatChem*, 2013, **5**, 1024-1031.
22. M. Opanasenko, A. Dhakshinamoorthy, M. Shamzhy, P. Nachtigall, M. Horáček, H. Garcia and J. Čejka, *Catal. Sci. Technol.*, 2013, **3**, 500-507.
23. A. Dhakshinamoorthy, M. Opanasenko, J. Čejka and H. Garcia, *Catal. Sci. Technol.*, 2013, **3**, 2509-2540.
24. W. M. Xuan, C. F. Zhu, Y. Liu and Y. Cui, *Chem. Soc. Rev.* 2012, **41**, 1677-1695.
25. L. F. Song, J. Zhang, L. X. Sun, F. Xu, F. Li, H. Z. Zhang, X. L. Si, C. L. Jiao, Z. B. Li, S. Liu, Y. L. Liu, H. Y. Zhou, D. L. Sun, Y. Du, Z. Cao and Z. Gabelica, *Energy Environ. Sci.*, 2012, **5**, 7508-7520.
26. I. Senkovska and S. Kaskel, *Chem. Commun.*, 2014, **50**, 7089-7098.
27. X. S. Wang, S. Q. Ma, D. F. Sun, S. Parkin and H. C. Zhou, *J. Am. Chem. Soc.*, 2006, **128**, 16474-16475.
28. Q. R. Fang, G. S. Zhu, Z. Jin, Y. Y. Ji, J. W. Ye, M. Xue, H. Yang, Y. Wang and S. L. Qiu, *Angew. Chem. Int. Ed.*, 2007, **46**, 6638-6642.
29. N. Klein, I. Senkovska, K. Gedrich, U. Stoeck, A. Henschel, U. Mueller and S. Kaskel, *Angew. Chem. Int. Ed.*, 2009, **48**, 9954-9957.
30. K. C. Wang, D. W. Feng, T. F. Liu, J. Su, S. Yuan, Y. P. Chen, M. Bosch, X. D. Zou and H. C. Zhou, *J. Am. Chem. Soc.*, 2014, **136**, 13983-13986.
31. D. Zhao, D. Q. Yuan, D. F. Sun and H. C. Zhou, *J. Am. Chem. Soc.*, 2009, **131**, 9186-9188.
32. D. Q. Yuan, D. Zhao, D. F. Sun and H. C. Zhou, *Angew. Chem. Int. Ed.*, 2010, **49**, 5357-5361.
33. H. X. Deng, S. Grunder, K. E. Cordova, C. Valente, H. Furukawa, M. Hmadeh, F. Gándara, A. C. Whalley, Z. Liu, S. Asahina, H. Kazumori, M. O'Keeffe, O. Terasaki, J. F. Stoddart and O. M. Yaghi, *Science*, 2012, **336**, 1018-1023.

34. L. G. Qiu, T. Xu, Z. Q. Li, W. Wang, Y. Wu, X. Jiang, X. Y. Tian and L. D. Zhang, *Angew. Chem. Int. Ed.*, 2008, **47**, 9487-9491.
35. J. Górka, P. F. Fulvio, S. Pikus and M. Jaroniec, *Chem. Commun.*, 2010, **46**, 6798-6800.
36. L. H. Wee, C. Wiktor, S. Turner, W. Vanderlinden, N. Janssens, S. R. Bajpe, K. Houthoofd, G. Van Tendeloo, S. De Feyter, C. E. A. Kirschhock and J. A. Martens, *J. Am. Chem. Soc.*, 2012, **134**, 10911-10919.
37. J. Reboul, S. Furukawa, N. Horike, M. Tsotsalas, K. Hirai, H. Uehara, M. Kondo, N. Louvain, O. Sakata and S. Kitagawa, *Nat. Mater.*, 2012, **11**, 717-723.
38. L. B. Sun, J. R. Li, J. Park and H. C. Zhou, *J. Am. Chem. Soc.*, 2012, **134**, 126-129.
39. D. Q. Yuan, D. Zhao, D. J. Timmons and H. C. Zhou, *Chem. Sci.*, 2011, **2**, 103-106.
40. T. Li, M. T. Kozlowski, E. A. Doud, M. N. Blakely and N. L. Rosi, *J. Am. Chem. Soc.*, 2013, **135**, 11688-11691.
41. M. Klimakow, P. Klobes, A. F. Thünemann, K. Rademann and F. Emmerling, *Chem. Mat.*, 2010, **22**, 5216-5221.
42. R. E. Morris and J. Čejka, *Nat. Chem.*, 2015, **7**, 381-388.
43. J. Park, Z. Y. U. Wang, L. B. Sun, Y. P. Chen and H. C. Zhou, *J. Am. Chem. Soc.*, 2012, **134**, 20110-20116.
44. Y. Y. Liu, J. R. Li, W. M. Verdegaal, T. F. Liu and H. C. Zhou, *Chem.-Eur. J.*, 2013, **19**, 5637-5643.
45. G. Barin, V. Krungleviciute, O. Gutov, J. T. Hupp, T. Yildirim and O. K. Farha, *Inorg. Chem.*, 2014, **53**, 6914-6919.
46. S. Marx, W. Kleist and A. Baiker, *J. Catal.*, 2011, **281**, 76-87.
47. Z. L. Fang, J. P. Dürholt, M. Kauer, W. H. Zhang, C. Lochenie, B. Jee, B. Albada, N. Metzler-Nolte, A. Pöppl, B. Weber, M. Muhler, Y. M. Wang, R. Schmid and R. A. Fischer, *J. Am. Chem. Soc.*, 2014, **136**, 9627-9636.
48. R. Q. Zhong, R. Q. Zou and Q. Xu, *Crystengcomm*, 2011, **13**, 577-584.
49. A. Schaate, P. Roy, A. Godt, J. Lippke, F. Waltz, M. Wiebcke and P. Behrens, *Chem.-Eur. J.*, 2011, **17**, 6643-6651.
50. Z. G. Hu, K. Zhang, M. Zhang, Z. G. Guo, J. W. Jiang and D. Zhao, *ChemSusChem*, 2014, **7**, 2791-2795.
51. J. L. C. Rowsell, A. R. Millward, K. S. Park and O. M. Yaghi, *J. Am. Chem. Soc.*, 2004, **126**, 5666-5667.
52. K. J. Kim, Y. J. Li, P. B. Kreider, C. H. Chang, N. Wannenmacher, P. K. Thallapally and H. G. Ahn, *Chem. Commun.*, 2013, **49**, 11518-11520.
53. F. Villemot, A. Galarneau and B. Coasne, *J. Phys. Chem. C*, 2014, **118**, 7423-7433.
54. M. J. Cliffe, W. Wan, X. D. Zou, P. A. Chater, A. K. Kleppe, M. G. Tucker, H. Wilhelm, N. P. Funnell, F. X. Coudert and A. L. Goodwin, *Nat. Commun.*, 2014, **5**, 4176.
55. A. Corma, *Chem. Rev.*, 1997, **97**, 2373-2419.
56. M. Tokunaga, J. F. Larrow, F. Kakiuchi and E. N. Jacobsen, *Science*, 1997, **277**, 936-938.
57. S. Horike, M. Dincă, K. Tamaki and J. R. Long, *J. Am. Chem. Soc.*, 2008, **130**, 5854-5855.
58. P. García-García, M. Müller and A. Corma, *Chem. Sci.*, 2014, **5**, 2979-3007.
59. H. Wu, Y. S. Chua, V. Krungleviciute, M. Tyagi, P. Chen, T. Yildirim and W. Zhou, *J. Am. Chem. Soc.*, 2013, **135**, 10525-10532.
60. O. Kozachuk, I. Luz, F. X. L. I. Xamena, H. Noei, M. Kauer, H. B. Albada, E. D. Bloch, B. Marler, Y. M. Wang, M. Muhler and R. A. Fischer, *Angew. Chem. Int. Ed.*, 2014, **53**, 7058-7062.

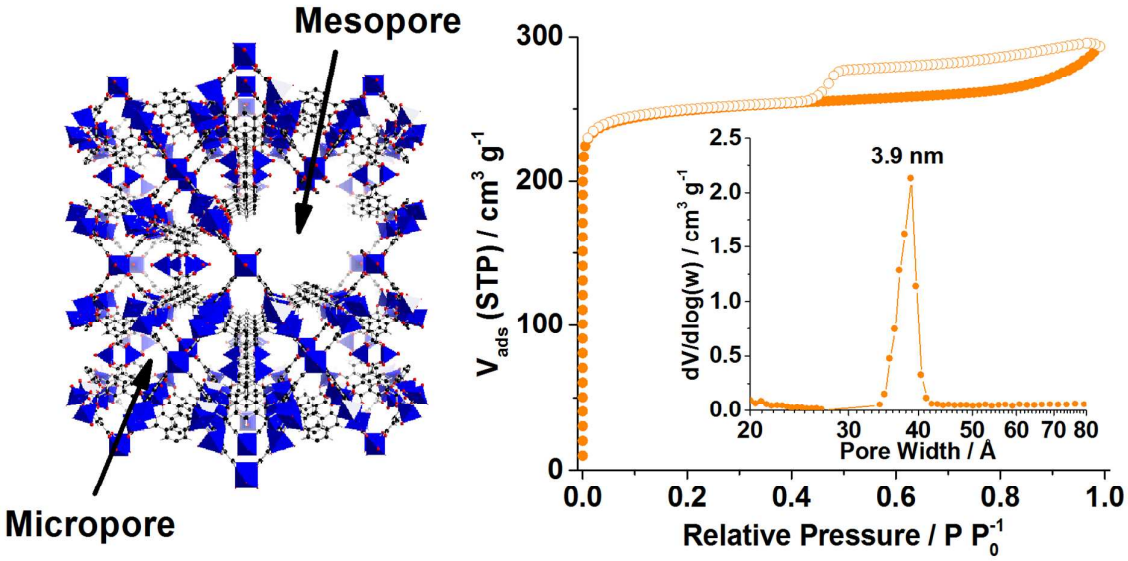

A hierarchical porous metal-organic framework CuBTC with mesopores of 3.9 nm has been facilely obtained as Lewis acid catalysts.